Study by X-Ray Tomography of the Mechanical Behavior of Concrete Foundations Affected by ASR

Sylvain Langlois, Amélie Fau, Maroua Maaroufi, Benjamin Smaniotto, Farid Benboudjema

Study by X-ray tomography of the mechanical behavior of concrete foundations affected by ASR

Sylvain Langlois[1], Amélie Fau[1], Maroua Maaroufi [1], Benjamin Smaniotto[1], Farid Benboudjema[1]

[1] Université Paris-Saclay, CentraleSupélec, ENS Paris-Saclay, CNRS, Laboratoire de Mécanique Paris-Saclay, 91190, Gif-sur-Yvette, France
sylvain.langlois@ens-paris-saclay.fr

Abstract. High-voltage electricity pylons are anchored in concrete foundations, which are mainly subjected to pull-out and compression loads. Under these loads, concrete aging and pathologies can lead to mechanical stability issue, and even failure. The alkali-silica reaction is a possible pathology that can be encountered in this type of structure. The aim of this work is to propose a method to analyze the mechanical behavior of the foundation affected by ASR under pylon pull-out. ASR is introduced, and an experimental protocol is proposed to create it in the mortar. A pylon pull-out test from a small-scale mortar foundation is carried out directly in an X-ray tomograph. This so-called in-situ test, coupled with computed tomography (CT), enables the force-displacement curve and failure modes to be analyzed. The test has already been carried out on sound mortar and will be extended to mortar affected by ASR. It will then be possible to deduce the influence of ASR on foundation failure modes.

Keywords: Concrete Foundation, Alkali-Silica-Reaction (ASR), In-situ Pull-out Test, Computed Tomography (CT)

1 Introduction

The construction of concrete foundations and the installation of pylons began in the early 20th century. These electricity pylons lie on concrete foundations consisting of a chimney and a succession of concrete slabs, as shown in Fig. 1.

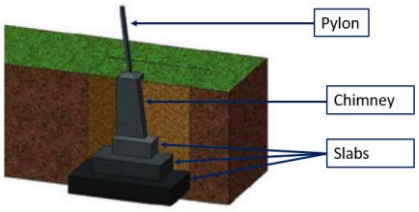

Fig. 1. Typical concrete foundations of high-voltage electricity pylons.

Under pull-out, concrete ageing and the development of pathologies can lead to mechanical instability problems up to failure. Alkali-silica-reaction (ASR) is a severe pathology that can be found in existing foundations.

Few studies have been carried out to predict the failure of concrete foundations under pylon pull-out, either experimentally or in terms of modeling and numerical simulations. Some authors (e.g. [1] and [2]) carried out pull-out or bending tests on a real scale, or slightly reduced scale, giving access to the load bearing capacity. These macroscopic data are then compared with the results of finite-element simulations. These studies (among others) did not include pathologies present in concrete, such as ASR. The mechanisms of ASR are now quite well studied. The amplitude and kinetics of the reaction depend on different criteria such as the chemical composition of the aggregates, granulometry, alkali content in the cement, liquid water saturation degree of the sample, and temperature, which has mainly a kinetic effect. The mechanical impact of ASR on concrete structures is still little known. [3] carried out the pull-out of a rebar from a concrete cube affected by ASR. The load and the cracking surface are analyzed for different stages of swelling. A finite element model combining damage mechanics and chemical swelling is used to simulate the test and validate the model. Similar studies have been carried out with different models, such as the Rigid Body Spring Model (RBSM) and the lattice discrete particle model [4]. However, these models are calibrated on macroscopic quantities and the results obtained on a microscopic scale (internal cracking, damage, displacement fields) are not verified. To better understand the mechanical impact of ASR, it is necessary to correlate the macroscopic and microscopic effects of the pathology.

This work develops a method for analyzing the mechanical impact of the pathology on the mechanical behavior of the foundation. Swelling due to ASR has been measured and its effect has been observed using X-ray tomography scans. An in-situ pylon pull-out test from a mortar foundation mock-up (1/50 scale) is then carried out in an X-ray tomograph. Computed Tomography allows microscopic observation of the degradation of the mortar foundation during the mechanical test. The mechanical test is carried out on sound mortar. The work will be extended to a foundation affected by ASR, whose development protocol is described in this paper.

2 Materials and methods

The scaled-down structure consists of a Glass Fiber Reinforced Polymer (GFRP) pylon and a mortar foundation. Two mortars are formulated. One contains reactive sands (ASR-M) to bring out ASR which is a 0.25-4mm siliceous limestone sand. The other mortar is non-reactive (NR-M) and contains 0-4mm limestone sand. The reference of the used cement is CEM II/A-LL 42.5R. The mortar formulations are shown in Table 1 and are manufactured following a ratio W/C=0.5 and a ratio S/C=3.

Table 1. Mix designs of the 2 mortars (NR-M and ASR-M).

Components	Density $[kg.m^{-3}]$	NR-M $[kg.m^{-3}_{mortar}]$	ASR-M $[kg.m^{-3}_{mortar}]$
Limestone sand 0-4 mm	2670	1517	0
Limestone sand 0,25-4 mm	2680	0	758
Siliceous limestone sand 0,25-4 mm	2680	0	758
Cement	3110	511	511
Water	1000	256	256

3 Experimental investigation of alkali-silica reaction

Protocols (inspired from [5]) were carried out to create the ASR. Each protocol is applied to three 4x4x16 cm mortar prisms. The amount of alkali in the cement is $Na_2O_{eq} = 0.94\%\ m_{cement}$. According to [6], the amount of soluble silica in sand is around 5%. NR-M prisms are cured in autogenous cure at 20°C. 4 protocols are investigated to create ASR. In each of them, alkalis are added to mixing water with 1M sodium hydroxide. Protocols are described below:

- ASR-M-1: autogenous cure at 20°C.
- ASR-M-2: 28 days autogenous cure at 20°C then cured in a 0.5 M NaOH at 34°C.
- ASR-M-3: cure in 1 M NaOH at 34°C.
- ASR-M-4: cure in 1 M NaOH at 60°C.

3.1 Longitudinal swelling measurements

Longitudinal swelling and mass evolutions are measured during the reaction (see Fig. 2 and Fig. 3). Both NR-M and ASR-M-1 undergo slight shrinkage. This may be due to loss of mass during autogenous cure which is 0.3% for NR-M and 0.22% for ASR-M-1. ASR-M-2 shrinks also during the 28 days endogenous cure. After immersion in NaOH, rapid elongation is measured. This may be due to the water absorption. After that, more longitudinal swelling is generated due to ASR. The same evolution can be seen on ASR-M-3 prisms with a higher amplitude. Among all the protocols, the cure at 60°C (ASR-M-4) generated the most swelling strains. At 91 days, a strain of 5000

µm/m, i.e. 0.5%, was measured. This elongation is correlated to the mass gain which is 2.9%. This protocol has been selected to create ASR.

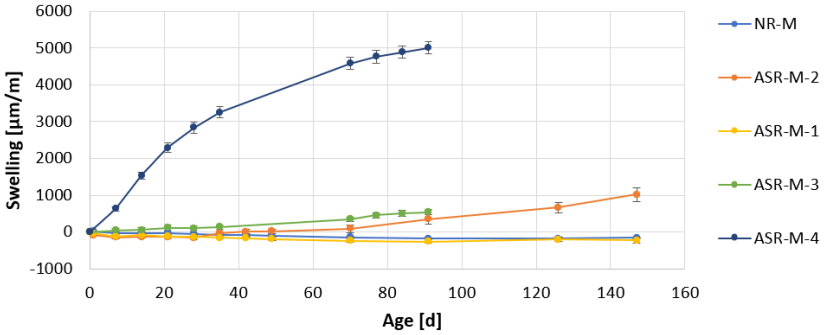

Fig. 2- Swelling of 4x4x16cm mortar specimen

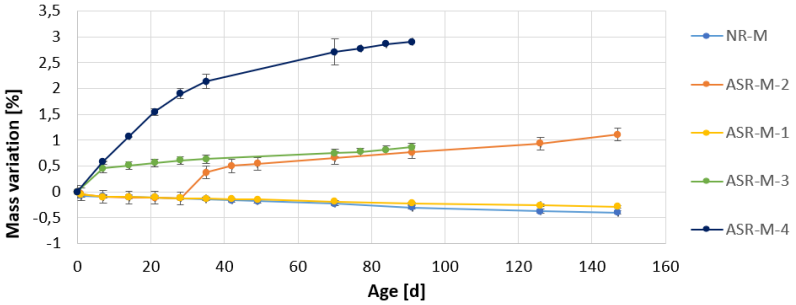

Fig. 3- Mass variation of 4x4x16cm mortar specimen

3.2 Computed tomography on ASR affected mortar

Scans were taken on an X-ray tomograph on a NR-M prism aged of 152 days and an ASR-M-4 prism aged of 96 days affected by ASR. Resolution is 39.3 µm. Fig. 4 shows 2D views of those scans. The view represents the cut of a 4x4x16 cm prism. Porosity, both reactive and non-reactive sand and cement paste can be seen on those views. On the ASR-M-4 scan, water can be seen inside the porosity as it was immersed in sodium hydroxide. More aggregates can be seen inside the affected mortar since the granulometry of the reactive sand is different of the non-reactive one. 33% of non-reactive sands were removed when sieved at 0.25mm while it was only 13% for reactive sands. Microscopic cracks are visible on mortar affected by ASR. Those cracks take place both in aggregate and cement paste. [7] has carried out observations on a mortar affected by ASR with SEM microscopy. It has been proposed that ASR products and cracks originate inside the aggregate and extend to the cement paste. Since the specimens are kept at 60°C, cracks can also be induced by incompatible thermal strain between cement paste and aggregates. However, it is unlikely that this may cause cracking going through the aggregates.

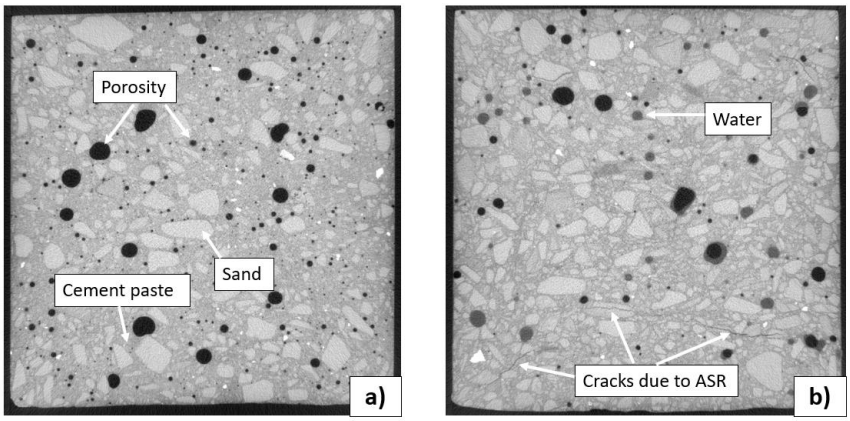

Fig. 4. a) 2D view of a scan on a sound mortar. b) 2D view of a scan on an ASR affected mortar

4 In-situ pull-out test on a sound mortar foundation

To understand the impact of ASR on the bear loading capacity of the foundation and the mode of failure, a mechanical test is proposed. An in-situ pylon pull-out test from a mortar foundation mock-up (1/50 scale) is carried out in an X-ray tomograph. For this first test, the mortar is not affected by the ASR.

4.1 Experimental set-up

The dimensions of the model and the test stand are shown in Fig. 5. The pylon is sealed into the mortar. The bottom of the foundation is glued directly into a collar, which is screwed to the testing machine. A clamp tights the pylon, which is also pinned to the testing machine. The test machines' upper part is fixed ($\delta_v = 0$), and the lower part can be moved downwards to apply the boundary conditions illustrated in Fig. 5.

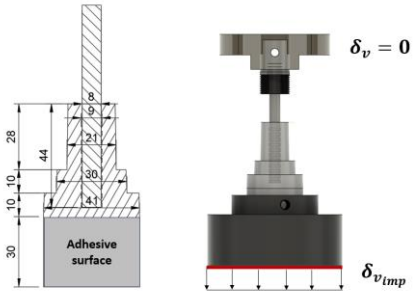

Fig. 5. Dimensions and boundary conditions of the experimental set-up

4.2 In-situ mechanical test

The foundation is loaded in steps. The loading curve for the in-situ pull-out test is shown in Fig. 6, with a test loading speed of 5µm/s. At each step, a scan is performed. This makes it possible to visualize the microstructure during mechanical loading. Each CT scan is taken from 1200 projections, with a scan duration of 30 minutes. The displacement displayed is a machine displacement.

A preload of 50N is applied to ensure contact between all parts of the set-up. Before each scan, a pause is marked to allow the specimen to relax. Scan0 is the reference scan, considered without mechanical load. An initial stress drop is visible between scan1 and scan2, corresponding to cracking located in the chimney-slab1 collar (see thereafter). This is followed by a brittle failure after scan3. Scan4 is a post-mortem scan.

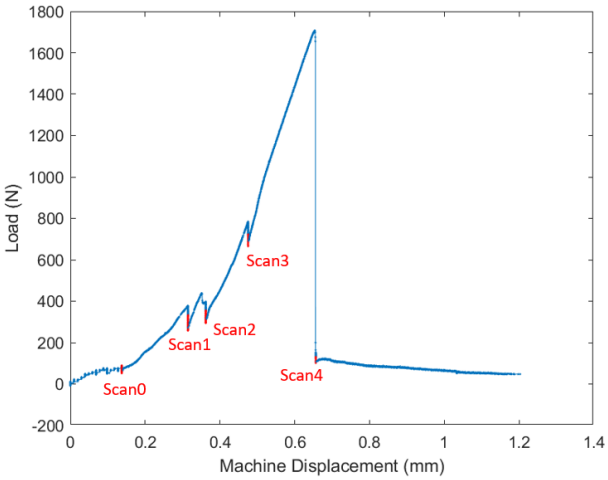

Fig. 6. Pull-out force and machine displacement during the in-situ pull-out test

4.3 Computed tomography on a sound foundation

Fig 7 shows a cross-section (Oxz) of scans 0, 2 and 4. The size of a voxel is 45µm. First of all, we can note the presence of artifacts. At the top of the image, a cone effect is visible. This artifact can be removed by reducing the detector-to-X-ray emitter distance and cropping the scan into the zone of interest.

Scan 0 is taken at the start of the test with preloading. Scan 2 is taken after a load of 430N. At this load, the chimney-slab collar failed. The crack is visible on scan 2. The crack starts at the pylon and propagates through the mortar, particularly in the pores (weakest region). Scan 4 is a scan taken just after the structure failed. We can see that the cracking at the chimney-slab1 collar has opened up, and below this cracking plane we can observe decohesion of the pylon-mortar interface. A second fracture occurs at the slab1-slab2 collar. These scans show that the crack spreads in the mortar through defects such as porosity, the interfacial transition zone (ITZ) and sometimes through the aggregates.

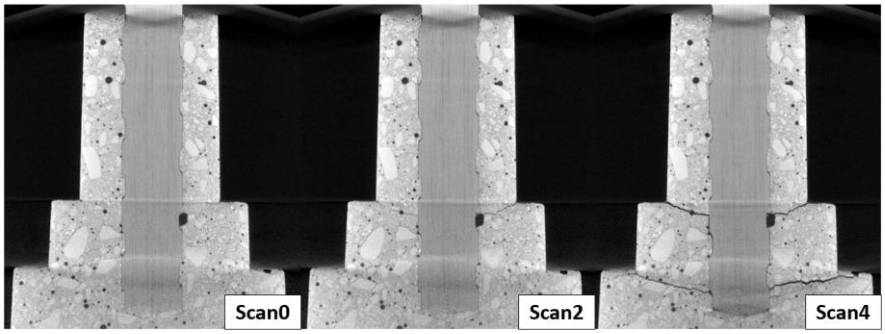

Fig 7. CT scans 0, 2 and 4 of the in-situ pull-out test on a sound mortar

5 Conclusion

This work aims to understand the impact of ASR on the mechanical behavior of the concrete foundation/pylon system submitted to pull-out. To this end, a protocol was successfully developed to accelerate the alkali-silica reaction in a 0,25-4mm mortar. A new experimental setup has been developed to test a reduced-scale mock-up of a pylon/mortar foundation system. CT is used to monitor the microstructure of the mock-up during mechanical loading. A first test was successfully carried out on a sound foundation. Results show that failure is intrinsic to the mortar foundation. Cracking starts to develop at the chimney-slab collar for a pull-out force of about 400N. Complete failure is then reached by cracking of the slab1-slab2 collar at pull-out force of about 1700N. The same test will be carried out on a foundation affected by ASR at different stages of swelling (30%, 60% and 100% of the total swelling strain) to observe and analyze the mechanical impact of the pathology on the failure mode and the load bearing capacity of the foundation.

This study will be extended using Digital Volume Correlation (DVC) to measure the displacement field of the sample during the test. This field will give access to information regarding the decohesion of the pylon-foundation interface, as it has been done by [8], and to the damage in the foundation. The mechanical impact of ASR can thus be analyzed on both macroscopic and microscopic scales.

Acknowledgments

This research was partly funded by the French National Research Agency (ANR) under the “HEAT COFFEE” project (grant “ANR-22-CHIN-0007-01”) and the Electricity Transport Network company (RTE).

References

1. Saito S, Kamimoto T, Yui K: Experimental and analytical study on anchorage capacity between single-pole tower and RC foundation. Oh, B.H., O.C. Choi, L. Chung and K. Concrete Institute (Eds.). Fracture Mechanics of Concrete and Concrete Structures 2010, Assessment, Durability, Monitoring and Retrofitting of Concrete Structures, pp 843–851. Korea, Seoul (2010)

2. Vivek B, Sharma S, Raychowdhury P, Ray-Chaudhri S: A study on failure mechanism of self-supported electric poles through full-scale field testing. Engineering Failure Analysis 77, 102–117 (2017)

3. Li P, Tan N, An X, Maekawa K, Jiang Z: Restraint Effect of Reinforcing Bar on ASR Expansion and Deterioration Characteristic of the Bond Behavior. Journal of Advanced Concrete Technology 18, 192–210 (2020)

4. Luo J, Wang Y, Asamoto S, Nagai K: Mesoscopic simulation of crack propagation and bond behavior in ASR damaged concrete with internal/external restraint by 3D RBSM. Cement and Concrete Composites 129, 104488 (2022)

5. Multon S, Cyr M, Sellier A, Leklou N, Petit L: Coupled effects of aggregate size and alkali content on ASR expansion. Cement and Concrete Research 38, 350–359 (2008)

6. Gao XX, Cyr M, Multon S, Sellier A: A comparison of methods for chemical assessment of reactive silica in concrete aggregates by selective dissolution. Cement and Concrete Composites 37, 82–94 (2013)

7. Tapas MJ, Sofia L, Vessalas K, Thomas P, Sirivivatnanon V, Scrivener K: Efficacy of SCMs to mitigate ASR in systems with higher alkali contents assessed by pore solution method. Cement and Concrete Research 142, 106353 (2021)

8. Jänicke G, Vintache A, Smaniotto B, Fau A, Farina I, Fraternali F, Hild F: Debonding analysis via digital volume correlation during in-situ pull-out tests on fractal fibers. Composites Part C: Open Access 9, 100302 (2022)